2022

Development of an Improved Mathematical Representation which Captures the Nonlinear Dynamic Behavior of a Drill-string Assembly

Eleazar Marquez
The University of Texas Rio Grande Valley, eleazar.marquez01@utrgv.edu

Proceedings of the ASME 2022
International Mechanical Engineering Congress and Exposition
IMECE2022
October 30 – November 3, 2022, Columbus, OH, USA

IMECE2022-95551

DEVELOPMENT OF AN IMPROVED MATHEMATICAL REPRESENTATION WHICH CAPTURES THE NONLINEAR DYNAMIC BEHAVIOR OF A DRILL-STRING ASSEMBLY

Eleazar Marquez[1]

[1]The University of Texas Rio Grande Valley, Edinburg, TX, USA

ABSTRACT

In this study, an improved mathematical representation of a drill-string assembly is developed to provide an alternative assessment on vibration irregularities proliferating downhole due to bit-rock interference. Lateral vibrations receive particular attention due to their high frequency content which alter the dynamic response of the drill-string, instigate casing damage, and impede optimal penetration rates. The response of the drill-string is captured by synthesizing compatible stationary bit excitations, via an auto-regressive digital filter, and implementing Monte Carlo simulation, while the power spectral density function is approximated to elucidate the dynamic characteristics during drilling. Formulating adequate physical parameters for the equation of motion implies incorporating a finite element technique, where the flexibility of the drill-string and elastic characteristics of the well-bore are accounted for. In conjunction with the stochastic nature of the excitation, the mathematical representation accounts for rig structural parameters, drilling fluid circulating within annulus/casing extremities, and a nonlinearity exhibited through a contact force generated between the well-bore and drill-string segment. To address the nature of the nonlinearity, the method of statistical linearization is incorporated to establish an equivalent linear system.

Keywords: Stochastic, nonlinear, Monte Carlo simulation, statistical linearization

NOMENCLATURE

Place nomenclature section, if needed, here. Nomenclature should be given in a column, like this:

α	alpha
β	beta

1. INTRODUCTION

1.1 Drill-string Assembly

In drilling, a drill-string assembly is primarily arranged of drill-pipe and drill-collar segments of uniform thickness and length (Figure 1). The diameter and strength characteristics of drill-collars are larger and are positioned at the lower section of the drill-string to provide the necessary weight-on-bit (WOB) requirements [3],[11]. The drill-string assembly is operated in tension-mode in order to eliminate irregularities such as buckling and fatigue irregularities. Depending on the type of rock formation, various types of fluids (e.g., known as *mud*) are utilized as lubricants during drilling procedures to extract rock debris towards the rig-surface and maintain stable operations [5],[12]. Besides drill-pipes and drill-collars, the drill-string assembly contains a critical component at the lower tip known as drill-bit, which is necessary to perforate through the formation. Generally, three types of drill-bits are widely used in industry, polycrystalline diamond compact (PDC) bits, roller cone bits, and fixed cutter bits [5],[9].

1.2 Drilling Vibrations

Geometrical variations generated from bit-rock interaction induce erratic vibration patters (e.g., axial, torsional, lateral, and parametric coupling oscillations) that alter the dynamic response of the drill-string and severely damage drilling equipment [1]. Several factors that yield undesired drilling conditions include premature bit-wear, whirling patterns, and casing damage effectuate from mass imbalance and axial misalignment variations [2]. The bouncing of the kelly (e.g., rig floor) and the whipping of the hoisting mechanism are indicatives of axial vibrations generated downhole [3],[4]. Further, a reduction between torsional energy and angular velocity generates drag effects, hole constrictions, key-seatings, and abrupt weight-on-bit (WOB) modulations. Such effects produce a stick-slip phenomenon and a rapid attenuation of the drill-bit [2],[5].

1.3 Research Motivation

Despite the manifestation of axial and torsional vibrations in the drill-string assembly, lateral vibrations represent the most aggressive and disruptive type oscillatory patterns in drilling, which exposes drilling equipment to excessive deterioration [5]. Widely referred as bending, transverse, or flexural vibrations, lateral vibrations remain the focal point of drill-string breakdowns given their high frequency characterization and ability to deviate drill-string trajectories [5].

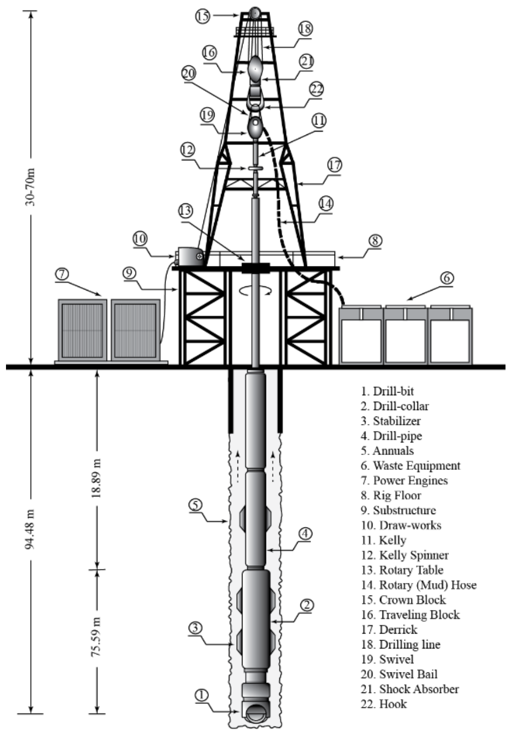

Figure 1. Rig Assembly

Thus, understanding vibration phenomena remains an imperative task due to the stochastic nature of the bottom-hole assembly (BHA). In this study, the stochastic nature of bit-rock interaction is addressed by proposing an alternative mathematical representation which accounts for stationary bit-excitations and elucidates the physical characteristics of the well-bore and drill-string assembly. Particularly, a target spectrum was incorporated to replicate the performance of a PDC drill-bit which generates frequency content near a rotational driving frequency, and thus time-histories were synthesized by passing white-noise via an auto-regressive digital filter. The improved mathematical representation accounts for rig structural parameters, drilling fluid circulating within annulus and casing extremities, and a nonlinearity exhibited through a contact alacrity between the well-bore and drill-string segment, capturing the salient features of the BHA.

2. MATHEMATICAL FORMULATION

In this study, Euler-Bernoulli beam theory, which assumes a small angle approximation, was adopted to model the drill-string assembly under the presence of lateral excitations. A multi-degree-of-freedom finite element model was proposed to establish a complete mathematical representation of the governing equation of motion (EOM) and quantify for its physical parameters [15]. Specifically, a two-node element containing three displacements and rotations per node is incorporated to describe the rig-suspended drill-string as a uniform, elastic beam (Figure 2). It was assumed that the beam element was a straight bar of uniform cross-section capable of resisting torques about its centroidal axis, axial forces, and bending moments about the two principal axes in the plane of its cross-section [15].

Upon implementing the finite-element discretization technique, the method of weighted residuals, also known as the Global Galerkin Method, allowed for an accurate derivation of the element stiffness and mass matrices.

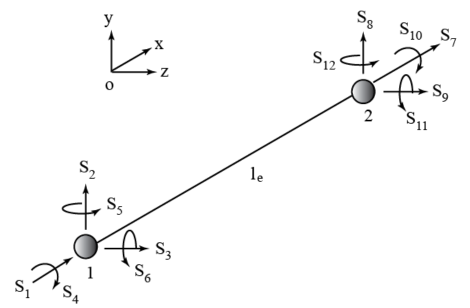

Figure 2. Node element, three displacements and three rotations

As loading conditions intensify and induce significant structural deformation, solutions to the governing matrix equations are no longer obtained explicitly by the linear relationship **P** = **KX** between the applied forces **P** and displacements **X** [15]. Instead, an iterative procedure, via a sequence of linear steps, was implemented to capture the high-amplitude displacements manifested within the assembly, where each step was characterized by a load increment. By executing the iterative process, nonlinear terms in the strain-displacement equations modified the element stiffness matrix by combining the standard elastic matrix, which is determined for the element geometry at the initial step, and the geometrical stiffness matrix, which depends on the element geometry and internal forces dwelling at the initial step. Therefore, the [symmetric] element stiffness matrix was established as

$$\mathbf{K} = \begin{bmatrix} k_1 & 0 & 0 & 0 & 0 & 0 & -k_1 & 0 & 0 & 0 & 0 & 0 \\ 0 & k_2 & 0 & 0 & 0 & k_3 & 0 & -k_2 & 0 & 0 & 0 & k_3 \\ 0 & 0 & k_2 & 0 & -k_3 & 0 & 0 & 0 & -k_2 & 0 & -k_3 & 0 \\ 0 & 0 & 0 & k_5 & 0 & 0 & 0 & 0 & 0 & k_5 & 0 & 0 \\ 0 & 0 & -k_3 & 0 & k_4 & 0 & 0 & 0 & k_3 & 0 & k_4 & 0 \\ 0 & k_3 & 0 & 0 & 0 & k_4 & 0 & -k_3 & 0 & 0 & 0 & k_4 \\ -k_1 & 0 & 0 & 0 & 0 & 0 & k_1 & 0 & 0 & 0 & 0 & 0 \\ 0 & -k_2 & 0 & 0 & 0 & -k_3 & 0 & k_2 & 0 & 0 & 0 & -k_3 \\ 0 & 0 & -k_2 & 0 & k_3 & 0 & 0 & 0 & k_2 & 0 & k_3 & 0 \\ 0 & 0 & 0 & k_5 & 0 & 0 & 0 & 0 & 0 & k_5 & 0 & 0 \\ 0 & 0 & -k_3 & 0 & k_4 & 0 & 0 & 0 & k_3 & 0 & k_4 & 0 \\ 0 & k_3 & 0 & 0 & 0 & k_4 & 0 & -k_3 & 0 & 0 & 0 & k_4 \end{bmatrix} \quad (1)$$

$$k_1 = \frac{EA}{L_e}\ ;\ k_2 = \frac{12EI_z}{L_e^3} + \frac{6P}{5L_e}; k_3 = \frac{6EI_z}{L_e^2} + \frac{P}{10};$$

$$k_4 = \frac{4EI_y}{L_e} + \frac{2L_eP}{15};\ k_5 = \frac{2EI_y}{L_e} - \frac{LP}{30} k_6 = \frac{GJ}{L_e}$$

where E represents the modulus of elasticity of drill-pipe and drill-collar segments, A the cross-sectional area, L_e the element length, I_y and I_z the moment of inertia of the element about the respective axes, P the axial load for WOB conditions, JG the torsional stiffness, J being the second moment of area, and G the shear modulus. By considering the inertial forces acting on the structure, nonlinear terms in the impulse-momentum equations modified the element mass matrix through the combination of the standard and geometrical mass matrices, yielding the following symmetric array

$$\mathbf{M} = \begin{bmatrix} \frac{m_e}{3} & 0 & 0 & 0 & 0 & 0 & \frac{m_e}{6} & 0 & 0 & 0 & 0 & 0 \\ 0 & m_1 & 0 & 0 & 0 & m_2 & 0 & m_3 & 0 & 0 & 0 & -m_4 \\ 0 & 0 & m_1 & 0 & -m_2 & 0 & 0 & 0 & m_3 & 0 & m_4 & 0 \\ 0 & 0 & 0 & m_7 & 0 & 0 & 0 & 0 & 0 & m_8 & 0 & 0 \\ 0 & 0 & -m_2 & 0 & m_5 & 0 & 0 & 0 & -m_4 & 0 & -m_6 & 0 \\ 0 & m_2 & 0 & 0 & 0 & m_5 & 0 & m_4 & 0 & 0 & 0 & -m_6 \\ \frac{m_e}{6} & 0 & 0 & 0 & 0 & 0 & \frac{m_e}{3} & 0 & 0 & 0 & 0 & 0 \\ 0 & m_3 & 0 & 0 & 0 & m_4 & 0 & m_1 & 0 & 0 & 0 & -m_2 \\ 0 & 0 & m_3 & 0 & -m_4 & 0 & 0 & 0 & m_1 & 0 & m_2 & 0 \\ 0 & 0 & 0 & m_8 & 0 & 0 & 0 & 0 & 0 & m_7 & 0 & 0 \\ 0 & 0 & m_4 & 0 & -m_6 & 0 & 0 & 0 & m_2 & 0 & m_5 & 0 \\ 0 & -m_4 & 0 & 0 & 0 & -m_6 & 0 & -m_2 & 0 & 0 & 0 & m_5 \end{bmatrix} \quad (2)$$

$$m_1 = \frac{13M_t}{35} + \frac{6\rho I_z}{5L_e}; m_2 = \frac{11M_tL_e}{210} + \frac{\rho I_z}{10}$$

$$m_3 = \frac{9M_t}{70} - \frac{6\rho I_z}{5L_e}; m_4 = \frac{13M_tL_e^2}{420} - \frac{\rho I_y}{10}$$

$$m_5 = \frac{M_tL_e^2}{105} + \frac{2L_e\rho I_y}{15}; m_6 = \frac{M_tL^2}{140} - \frac{L\rho I_y}{30}$$

$$m_7 = \frac{\rho L_e J_x}{3}; m_8 = \frac{\rho L_e J_x}{6}$$

where ρ represents the density of the material, m_e the element mass, and M_t the total mass of the element, which consists of the drill-string mass M, the added-mass of the fluid M_c discharged into the casing, and the added-mass progressing through the annulus M_a [21]. Such expression is denoted as

$$M_t = M + M_c + c_m M_a \quad (3)$$

where c_m characterizes a coefficient which is a function of three parameters, e.g., radii of the well-bore, kinematic velocity of the mud, and [circular] frequency of the displacement. Therefore, assembling element matrices generated a complete MDOF representation of the drill-string as

$$\mathbf{M}\ddot{\mathbf{x}}(t) + \mathbf{C}\dot{\mathbf{x}}(t) + \mathbf{K}\mathbf{x}(t) = \mathbf{g}(t) \quad (4)$$

where **M**, **C**, **K** denote the total mass, damping, and stiffness matrices, $\ddot{\mathbf{x}}(t), \dot{\mathbf{x}}(t)$, and $\mathbf{x}(t)$ characterize the acceleration, velocity, and displacement vectors as a function of time, respectively, and $\mathbf{g}(t)$ denotes the [stochastic] excitation applied on the drill-bit.

Although damping of structures is frequently depicted by approximate methods such as viscous damping, Rayleigh damping, modal damping, and augmented modal damping, its exact nature in complex structural systems remains oblivious [16]. In this study, a modal damping methodology is incorporated given its versatility of specifying damping factors for a specific number of modes. From the orthogonality property of modes and by assuming a complete NxN modal matrix, the physical damping matrix is established by the equation

$$\mathbf{C} = \sum_{r=1}^{N} \frac{2\zeta_r\omega_r}{M_r} (\mathbf{M}\boldsymbol{\phi}_r)(\mathbf{M}\boldsymbol{\phi}_r)^{\mathrm{T}} \quad (5)$$

where ζ_r represents the nonzero [damping] modes, assumed to be $\zeta_r = 0.06$, M_r is the modal mass matrix, ϕ_r the eigenvectors, and ω_n the natural frequency of each mode. Establishing a complete mathematical representation also inquires considering the sustained interaction between the drill-string and well-bore via a Hertzian contact law **F**, which assumes that the lateral deflection of the assembly remains constrained until a clearance threshold is exceeded [13],[17-20]. As a result, a nonlinearity is introduced into the governing equations of motion as

$$\mathbf{M}\ddot{\mathbf{x}}(t) + \mathbf{C}\dot{\mathbf{x}}(t) + \mathbf{K}\mathbf{x}(t) + \mathbf{F}(\mathbf{x}(t)) = \mathbf{g}(t) \quad (6)$$

where $\mathbf{F}(\mathbf{x}(t))$ models the influence of the rock. Such interaction is described as

$$\mathbf{F}(\mathbf{x}_i(t)) = \begin{cases} k(x_i(t) + a)^{3/2} & x \le a \\ 0 \quad -a \le x \le a & i = 1,2,3, \ldots N-1 \\ k(x_i(t) - a)^{3/2} & x \ge a \end{cases} \quad (7)$$

where k denotes the elasticity of the formation, a characterizes the clearance value, and N is the total number of degrees-of-freedom. It is depicted in Figure 2 that the elasticity of the formation influences the development of the nonlinearity.

In this study, a probabilistic approach was adopted to provide necessary frequency content for a PDC drill-bit and determine the response of the drill-string assembly. A double-sided power spectrum was specifically incorporated to replicate the performance of the bit which generates frequency content near a rotational driving frequency. By employing such spectrum and passing white noise through an auto-regressive (AR) digital filter, compatible stationary were synthesized, and thus a complete dynamic representation is established. The target spectrum is given by the equation

$$S(\omega) = S_0 \frac{1 + 4\zeta_g^2\left(\frac{\omega}{\omega_g}\right)^2}{\left[\left(1 - \left(\frac{\omega}{\omega_g}\right)^2\right)^2 + \left(2\zeta\frac{\omega}{\omega_g}\right)^2\right]} \quad (8)$$

where ζ_g and ω_g characterize the damping ratio and natural frequency, respectively. Specifically, $\zeta_g = 0.07$ and $\omega_g = 24.35$ rad/s are established for the development of the target spectrum represented in Figure 3. A scaling constant of $S_0 = 1.5x10^9$ is multiplied with the input process to maintain magnitude proximity with field data [13].

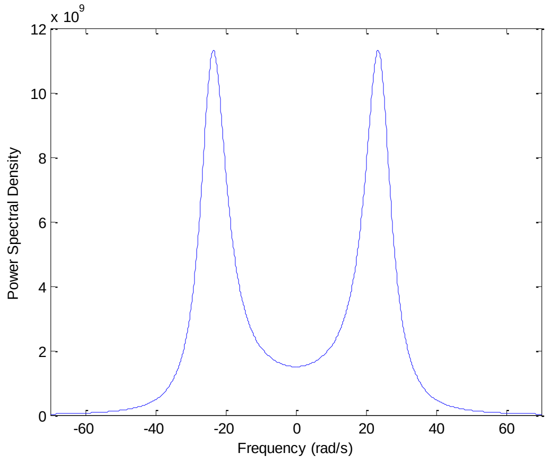

Figure 3. Two-sided auto-spectral density representing a PDC drill-bit excitation

For such stationary process, a total of 500 time histories were synthesized through a digital filter of order 100 containing a sampling rate $T = \pi/\omega_c$, 16384 data points, and a Nyquist frequency $\omega_c = 100$ rad/s. Figure 4, displays an acceleration record extracted from the ensemble of records and its random characteristics propagating as a function of time.

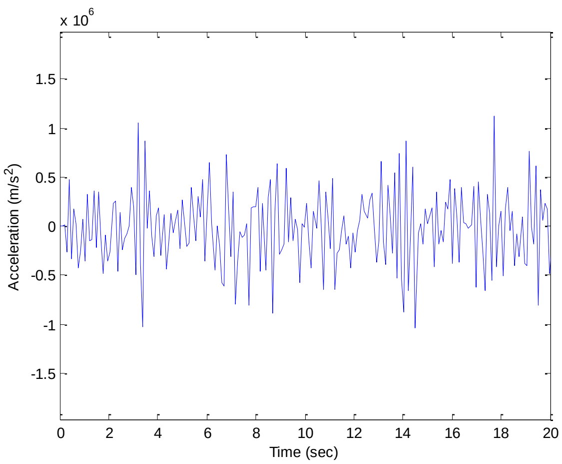

Figure 4. Synthesized time histories for stationary process versus time via an AR digital filter

Determining the response of the nonlinear MDOF system subject to a stochastic excitation implied implementing the method of statistical linearization, which offers a systematic scheme to delineate an approximate solution [24],[26]. Such method replaces the nonlinear dynamical system with an auxiliary set of linear equations and establishes an exact, analytical form of solution. Therefore, representing the nonlinear EOM in terms of an equivalent linear system was described as

$$\mathbf{M}\ddot{\mathbf{x}}(t) + \mathbf{C}\dot{\mathbf{x}}(t) + (\mathbf{K} + \mathbf{K_{eq}})\mathbf{x}(t) = \mathbf{g}(t) \tag{9}$$

where $\mathbf{K}_{eq}$ represents the equivalent stiffness matrix which was obtained by minimizing the difference $\boldsymbol{\varepsilon}$ between the actual and equivalent linear system. By applying the Euclidean norm, $\|\boldsymbol{\varepsilon}\|_2$, the minimum $\boldsymbol{\varepsilon}$ was defined as

$$\|\boldsymbol{\varepsilon}\|_2^2 = \boldsymbol{\varepsilon}^{\mathrm{T}}\boldsymbol{\varepsilon} = E\{\boldsymbol{\varepsilon}^{\mathrm{T}}\boldsymbol{\varepsilon}\} \tag{10}$$

where $\boldsymbol{\varepsilon}^{\mathrm{T}}$ indicates the transpose of the vector $\boldsymbol{\varepsilon}$. Therefore, the minimization criterion was satisfied by establishing the following condition

$$\frac{\partial}{\partial k_{ij}^{eq}} E\{\boldsymbol{\varepsilon}^{\mathrm{T}}\boldsymbol{\varepsilon}\} = 0 \tag{11}$$

where the elements k_{ij}^{eq} pertain to the equivalent matrix $\mathbf{K_{eq}}$. Substituting the linearity property of the expectation operator into the difference equation yielded the following expression

$$E\{x_j \Phi_i\} = \sum_{s=1}^{n} \left[k_{ij}^{eq} E[x_s x_j]\right] \tag{12}$$

As a result, obtaining a solution regarding the statistical linearization procedure involved establishing a specific probability density function to compute the mathematical expectation. A Gaussian zero-mean approximation was an adequate formulation in determining the elements of the equivalent linear system and guaranteeing a Gaussian response with the expression

$$\mathbf{K}_{ij}^{eq} = E\left\{\frac{\partial F}{\partial x}\right\} \tag{13}$$

Therefore, combining equations resulted in

$$\mathbf{K}_{ij}^{eq} = \frac{3k}{2\sqrt{2\pi\sigma_i}}\left[\int_{-x}^{a} (-x_i - a)^{\frac{1}{2}} e^{-x_i^2/2\sigma_i^2} dx_i + \int_{a}^{x} (x_i - a)^{\frac{1}{2}} e^{-x_i^2/2\sigma_i^2} dx_i\right] \tag{14}$$

3. RESULTS AND DISCUSSION

The improved drill-string representation subject to stationary excitations was compromised by a clamped suspension system, representative of rig-floor structural behavior, a drill-pipe, two drill-collars, and two stabilizers positioned 5 m and 24.5 m beneath the drilling surface, which preclude lateral mobility. Despite considering an assembly reduction to address computational power, the proposed drill-string length warranted sufficiency to evaluate and predict oscillatory phenomena. Physical quantities such as pipe length, diameter, and elastic properties are specified in Tables 1 and 2, and thus selected based on API standards.

3.1 Drill-string Parameters for Study

Particularly, a single element characterizes the suspension system, 12 elements of length 0.9144 m constitute the drill-pipe segment, and 21 elements of equivalent length compromise the drill-collar segments, resulting in a total of 198 degrees-of-freedom after matrix assemblage. However, capturing the drill-string response and approximating its power spectral features involves enforcing a constant compressive force of 10^4 N exclusively on the drill-collar segments to ensure appropriate management of WOB requirements.

After integrating the governing equations of motion, computing response estimates across the simulated ensemble was an imperative procedure to evaluate the accuracy of results and observe the oscillatory tendencies proliferating within the drilling assembly. For the stationary process, Figures 6 and 7 elucidate the lateral response characteristics proliferating as a function of time under a natural frequency of $\omega_0 = 7.65$ rad/s and $\omega_0 = 38.54$ rad/s, respectively.

Results revealed a maximum displacement of 0.02 m occurring adjacent to the BHA during a low frequency manifestation (Figure 5). However, given the progression of each natural frequency, a resonance phenomenon effectuated within the central and lower domains of the drill-string as the natural frequency equated the frequency of excitation, prompting abrupt and detrimental fluctuations exceeding 0.40 m (Figure 6). It was further observed that lateral discrepancies effectuated at the rig-floor, which gradually intensified given the natural frequency progression, was captured with the improved mathematical model, allowing [crew] members to evade any intolerable oscillatory materialization generated through specific operating frequencies.

Table 1. Drill-string quantities

Suspension System	
Mass	$2.376x10^4$ kg
Damping	$4.000x10^4$ $\text{Ns} \cdot \text{m}^{-1}$
Stiffness	$1.000x10^7$ $\text{N} \cdot \text{m}^{-1}$
Drill-pipe	
Total length	9.44 m
Inner diameter	0.105 m
Outer diameter	0.130 m
Drill-collar	
Total length	9.44 m
Inner diameter	0.105 m
Outer diameter	0.203 m

Table 2. Steel and drilling mud quantities

Steel	
Poisson's ratio	$3.300x10^{-1}$
Density	$7.830x10^3$ $\text{kg} \cdot \text{m}^{-3}$
Modulus of elasticity	$2.070x10^{11}$ Pa
Drilling Mud	
Casing	45.35 kg
Annulus	317.52 kg
Mud mass per meter	4.8005 kg
Mud constant	0.2 (DP) 1.5 (DC)

A further assessment included approximating the corresponding transfer function, via a Fourier transformation, to discern the frequency content of possible failure. For simplification purposes, the power spectral density function was exclusively predicted at a natural frequency of $\omega_0 = 7.65$ rad/s (Figure 7 and Figure 8). Results indicated that a stable drill-string operates within a frequency range of approximately 20-40 rad/s, which was equivalent to 3-6 Hz. However, as the natural frequency progressed to 24.35 rad/s, results indicated that the drill-string operated at approximately 50 rad/s, which could induce vibration irregularities due to resonance effects.

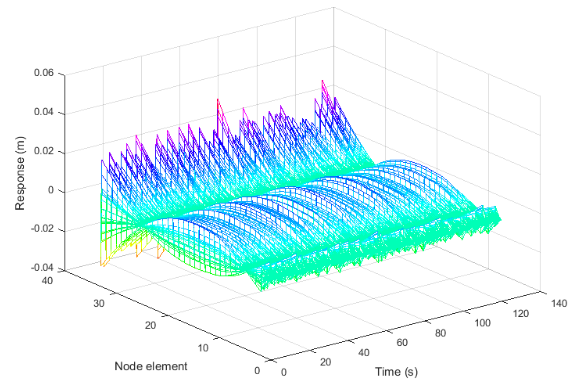

Figure 5. Time-domain response at $\omega_0 = 7.65$ rad/s

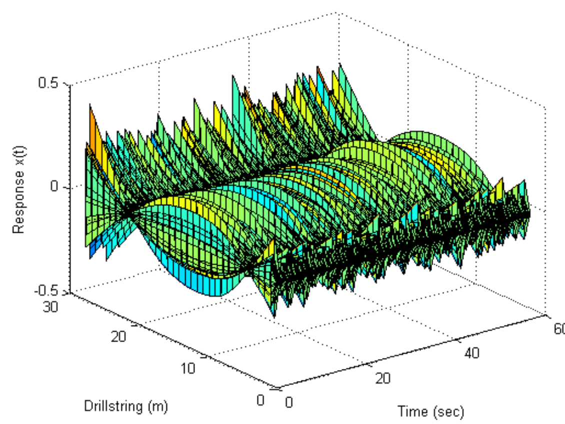

Figure 6. Time-domain response at $\omega_0 = 38.54$ rad/s

For both cases, however, slight spectrum variations were generated beyond 130 rad/s due to nature of the nonlinearity induced from a recurrent interaction between casing and well-bore extremities. Results additionally indicated that if the damping factor was increased to 0.4, the magnitude of the frequency content beyond 130 rad/s would decrease significantly. Nonetheless, the nonlinearity effects remained visible within the spectrum, but were insignificant.

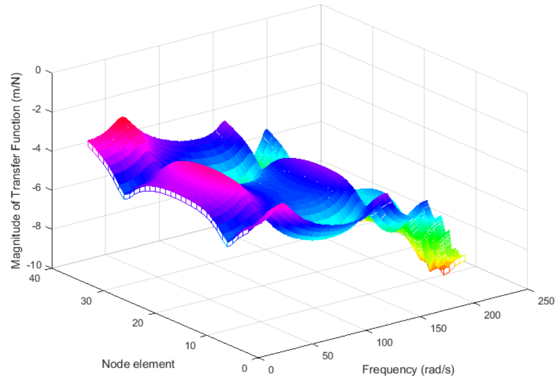

Figure 7. Power spectrum for $\omega_0 = 7.65$ rad/s

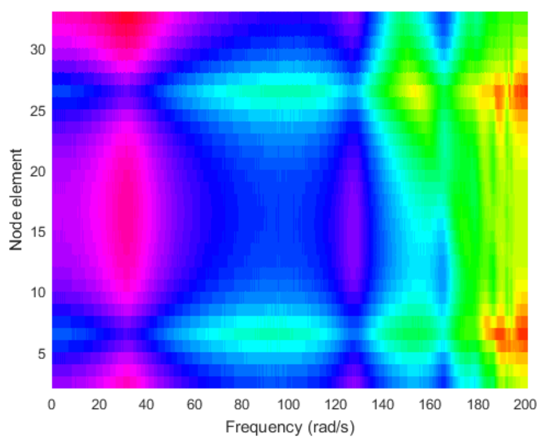

Figure 8. Two-dimensional spectrum of $\omega_0 = 7.65$ rad/s

4. CONCLUSION

Capturing the pragmatic response and power spectral density function of the suspended drill-string assembly was accomplished by proposing the incorporation of stationary excitations on the derived dynamical representation. Compatible time histories for a PDC drill-bit were synthesized by means of filtering a target spectrum via an AR digital filter to generate frequency content near a rotational driving frequency. Within the premises of the proposition, the improved mathematical representation accounted for rig structural parameters, drilling mud dispersed within annulus and casing extremities, a stiffness nonlinearity proliferating between the well-bore and drill-string marginal segment, and an axial load acting directly on the drill-collars. It provided a rigorous assessment on vibration irregularities proliferating at both ends of the drill-strings. Formulating adequate physical parameters for the governing equation of motion implied incorporating a finite-element technique, which accounted for the flexibility of the drill-string and elastic characteristics of the well-bore through six degrees-of-freedom per node.

Numerical results displayed a maximum displacement occurring within the BHA and minor discrepancies manifesting at the rig-floor during a low natural frequency operation. It was additionally observed that as the natural frequency equated the frequency of excitation, a dynamic response alteration was manifested throughout the central and lower segments of the drill-string, which exposed the assembly to various types of irregularities. Particularly, results inidcated a significant reduction in response at the drill-bit segment, e.g., approximately 0.02m, in comparison to Chevallier [13], which confirmed a maximum response of 0.6m with a fixed drill-string assembly and a finite element representation of four degrees-of-freedom per node. With the proposed mathematical representation, it is concluded that the response and power spectral density function yield acceptable approximations when applied to a relevant target spectrum.

REFERENCES

[1] A. Besaisow and M. Payne, "A study of excitation mechanisms and resonances inducing bottomhole-assembly vibrations," *SPE drilling engineering*, vol. 3, no. 1, pp. 93–101, 1988.

[2] M.P. Dufeyte and H. Henneuse, "Detection and monitoring of the slip-stick motion: Field experiments," in *SPE/IADC Drilling Conference*, 1991.

[3] D. Dareing, "Drill collar length is a major factor in vibration control," *Journal of petroleum technology*, vol. 36, no. 4, pp. 637–644, 1984.

[4] D. Dareing, "Rotary Speed, Drill Collars Control Drillstring Bounce," *Oil and Gas Journal*, vol. 81, no. 23, pp. 63–68, 1983.

[5] P.D. Spanos, A.M. Chevallier, N. P. Politis, and M. L. Payne, "Oil and Gas Well Drilling: A Vibrations Perspective," *The Shock and Vibration Digest*, vol. 35, no. 2, pp. 85–103, 2003.

[6] J.F. Brett, "The Genesis of Bit-Induced Torsional Drillstring Vibrations," *SPE Drilling Engineering*, vol. 7, no. 3, pp. 168–174, 1992.

[7] L.Van den Steen, "Surpressing Stick-Slip Induced Drillstring Oscillations: A Hyperstability Approach," Ph.D. Thesis, University of Twente, The Netherlands, 1997.

[8] K. Vandiver, J. Nicholson, and R.-J. Shyu, "Case studies of the bending vibration and whirling motion of drill collars," *SPE Drilling Engineering*, vol. 5, no. 4, pp. 282–290, 1990.

[9] J.F. Brett, T. M. Warren, S. M. Behr, and Amoco Production Co, "Bit Whirl-A New Theory of PDC Bit Failure," *SPE Drilling Engineering*, vol. 5, no. 4, pp. 275–281, Dec. 1990.

[10] R.-J. Shyu, "Bending Vibration of Rotating Drill Strings," Ph.D. Thesis, Massechusetts Institute of Technology, Cambridge, Mass., 1989.

[11] V.A. Dunayevsky, F. Abbassian, and A. Judzis, "Dynamic stability of drillstrings under fluctuating weight on bit," *SPE drilling & completion*, vol. 8, no. 2, pp. 84–92, 1993.

[12] J. D. Macpherson, J. S. Mason, and J. E. E. Kingman, "Surface Measurement and Analysis of Drillstring Vibrations While Drilling," in *SPE/IADC Drilling Conference*, 1993.

[13] A.M. Chevallier, “Nonlinear Stochastic Drillstring Vibrations,” Ph.D. Thesis, Rice University, Houston, Texas, 2000.

[14] J.L. Kennedy, *Fundamentals of Drilling - Technology and Economics*. Tulsa, Oklahoma: PennWell Books, 1983.

[15] J.S. Przemieniecki, *Theory of Matrix Structural Analysis*. Mineola, New York: Dover Publications, 1985.

[16] R.R. Craig Jr and A. J. Kurdila, *Fundamentals of Structural Dynamics*. 2nd ed. Hoboken, New Jersey: John Wiley & Sons, Inc., 2006.

[17] S.H. Crandall. Random Vibration of a Nonlinear System with a Set-up Spring. *Journal of Applied Mechanics, Transactions of the ASME*, 84:477-492, September 1962. Series E.

[18] H.-S. Jing and K.-C. Sheu. Exact Stationary Solutions of the Random Response of a Single-Degree-of-Freedom Vibro-Impact System. *Journal of Sound and Vibration*, 141(3): 363-373, 22 September 1990.

[19] H.-S. Jing and M. Young. Random Response of a Single-Degree-of-Freedom Vibro-Impact System with Clearance. *Earthquake Engineering and Structural Dynamics*, 19(6):789-798, August 1990.

[20] H.-S. Jing and M. Young. Impact Interactions between Two Vibration Systems under Random Excitation. *Earthquake Engineering and Structural Dynamics*, 20(7):667-681, July 1991.

[21] M.L. Payne, “Drilling Bottom-Hole Assembly Dynamics,” Ph.D. Thesis, Rice University, Houston, Texas, 2000.

[22] P.D. Spanos, J. Tezcan and P. Tratskas. Stochastic Processes Evolutionary Spectrum Estimation via Harmonic Wavelets. *Computer Methods in Applied Mechanics and Engineering*, 194:1367-1383, 8 April 2005.

[23] P.D. Spanos, “ARMA Algorithms for Ocean Wave Modeling,” *J. Energy Resour. Technol.*, vol. 3, pp. 300–309, Sep. 1983.

[24] J.B. Roberts and P.D. Spanos, *Random Vibration and Statistical Linearization*. Mineola, New York: Dover Publications, Inc., 1999.

[25] A.K. Chopra. Dynamics of Structures: *Theory and Applications to Earthquake Engineering*. 4th ed. Upper Saddle River, New Jersey: Prentice Hall, 2012.

[26] P.D. Spanos, A.M. Chevallier, and N. P. Politis, “Nonlinear Stochastic Drill-string Vibrations,” *Journal of Vibration and Acoustics*, vol. 124, pp. 512–518, 2002